Growth and Characterization of Fluorocarbon Thin Films Grown from Trifluoromethane (CHF$_3$) Using Pulsed-Plasma Enhanced CVD

EDMUND J. WINDER, KAREN K. GLEASON

Department of Chemical Engineering, Massachusetts Institute of Technology, Room 56-469, Cambridge, Massachusetts 02139

ABSTRACT: Trifluoromethane (CHF$_3$) was used as a precursor gas in pulsed-plasma enhanced CVD to deposit fluorocarbon films onto Si substrates. The film composition, as measured by X-ray photoelectron spectroscopy (XPS) of the $C1s$ peak, was observed to change as the plasma duty cycle was changed by varying the plasma off-time; this offers a route to control the molecular architecture of deposited films. FTIR results indicate that the film is primarily composed of CF$_x$ components, with little or no C—H incorporation into the film. The rms roughness of the films is extremely low, approaching that of the Si substrate; the low growth rate and consequent high-power input/thickness is believed to be partly responsible. CHF$_3$ produces films with higher % CF$_2$ compared to other hydrofluorocompound (HFC) monomers (CH$_2$F$_2$ and C$_2$H$_2$F$_4$). However, the deposition kinetics for all three HFC gases display similar trends. In particular, at a fixed on-time of 10 ms, the deposition rate per pulse cycle reaches a maximum at an off-time of approximately 100 ms. © 2000 John Wiley & Sons, Inc. J Appl Polym Sci 78: 842–849, 2000

Key words: trifluoromethane; pulsed plasma; fluorocarbon film; PECVD

INTRODUCTION

Fluorocarbon thin films are an area of active research because they can display a variety of desirable properties not easily obtained with other materials. Specifically, fluorocarbon thin films are being investigated for their use as "low-k" dielectric materials in semiconductor device fabrication,[1–3] as biocompatible coatings,[4–6] as hydrophobic, nonstick coatings,[7] and as low-friction coatings.[8,9] Plasma-enhanced CVD (PECVD) is an attractive deposition method for these films because it allows precise thickness control and, because it is solventless, greatly reduces environmental impact compared to traditional coating processes such as spin-on coating.[10] Pulsed-PECVD has advantages over continuous plasma CVD because the timing of the pulses provides the ability to tune the deposition process.[11,12] By varying the plasma duty cycle (the fraction of the cycle time during which the plasma is applied), the deposition can be tailored to make use of either the short-lived ionic species dominant in the plasma or the longer-lived radical and excited neutral species dominant when the plasma is off; this affects the chemical composition of the resulting film. This improved compositional control is reflected in a variation in the fluorine-to-carbon (F : C) ratio, with a corresponding change in film

properties. Additionally, reducing the proportion of plasma on-time reduces the ion bombardment of the growing surface, resulting in a less crosslinked film.

A variety of precursors have been employed to grow fluorocarbon films using PECVD and pulsed-PECVD, including CH_2F_2, $C_2H_2F_4$, and hexafluoropropylene oxide (HFPO).[4,13] These precursors were used because they were expected to produce difluorocarbene (CF_2) radicals to varying extents, based on their known thermal and photolytic decomposition pathways.[14,15] These difluorocarbene radicals are considered important for CF_2 chain growth.[16] In this article, we report on the growth and characterization of thin fluorocarbon films using another hydrofluorocompound precursor, trifluoromethane (CHF_3), that also produces difluorocarbene by pyrolysis.[17,18] Films were grown with this precursor at five different pulsed-plasma duty cycles and subsequently analyzed to determine their composition with X-ray photoelectron spectroscopy (XPS) and Fourier transform infrared spectroscopy (FTIR), their morphology with atomic force microscopy (AFM), and their wetting properties with contact-angle measurements.

EXPERIMENTAL

Pulsed-PECVD films were grown using five different duty cycles. The plasma on-time was fixed at 10 ms, while off-times of 20, 50, 100, 200, and 400 ms were used. These deposition conditions are referred to as 10/20, 10/50, 10/100, 10/200, and 10/400, respectively. The films were grown on Si substrates placed on the water-cooled ground electrode in a stainless-steel capacitively coupled cylindrical reactor chamber of about 6700-cm^3 volume containing 4-in. diameter electrodes spaced 1-in. apart. The plasma was produced by 13.56-MHz rf excitation at a maximum peak power of 280 W, while reflected power was minimized with a matching network. The trifluoromethane precursor was 98% pure and used as received from Lancaster. Reactor pressure was kept at 1 Torr during runs, and the feed gas flow rate was 12.5 standard cm^3 (sccm). Deposition times were 15 min unless otherwise indicated.

XPS survey scans and high-resolution $C1s$ spectra were obtained using a Physical Electronics 5200C spectrometer employing a Mg anode operating at 300 W. Further details of the XPS setup and $C1s$ peak least-squares nonlinear regression parameters were previously provided.[19]

Transmission FTIR spectra were obtained using a Nicolet Magna 860 spectrometer equipped with a DTGS KBr detector. A background spectrum taken with a bare Si wafer was subtracted from all of the film spectra. All samples were purged for 20 min with dry N_2 prior to collecting spectra in order to remove adsorbed water from the films. For each spectrum, 64 scans were averaged. Although sample film thicknesses varied, the resultant spectra were normalized to a "standard" thickness of 1500 Å to facilitate comparison.

AFM images were obtained at three different scales on each film: 2×2 μm, 1×1 μm, and 200×200 nm. AFM scans were performed in air using a Digital Instruments Nanoscope III scanning probe microscope operated in tapping mode with an etched Si cantilever tip. Although tapping-mode AFM does not provide as high a resolution as does contact mode AFM, it greatly reduces the likelihood of sample damage due to dragging the AFM tip across the polymer films.

Surface wetting was investigated by measuring the advancing and retreating contact angles of $\approx$ 5 μL water drops on the film surfaces using a Ramé–Hart manual goniometer. Measurements were made at three different points on each sample.

Film thicknesses were measured with contact profilometry and single-wavelength ellipsometry. Profilometry was performed with a Tencor P10 Profilometer equipped with a 2-μm radius-of-curvature diamond stylus. Ellipsometry measurements were taken using a Gaertner Scientific L116A ellipsometer operating at a wavelength of 632.8 nm (HeNe laser source) at an incident angle of 70°.

RESULTS AND DISCUSSION

Growth Rates

As mentioned above, depositions were performed at five different duty cycles. All but the lowest duty cycle, 10/400, were found to be effective in growing fluorocarbon films with this precursor. Although film growth was in some instances observed using a 10/400 duty cycle, it was difficult both to strike and to maintain a stable plasma; successful growth at this set of conditions required frequent tuning of the matching network.

Table I   CHF$_3$ Film Growth Rates

Plasma Conditions	Growth Rate (Å/s)	Growth Rate (Å/Cycle)
10/20	15.1	0.454
10/50	10.1	0.606
10/100	5.53	0.608
10/200	1.09	0.228
10/400	0.0839	0.0344

Growth rates of fluoropolymer films grown from CHF$_3$ at various plasma conditions. Rates are shown on a per-time and per-cycle basis.

Due to the low growth rates and instability of film growth at 10/400, we consider reproducible growth at these conditions to be problematic.

A series of films at the different duty cycles were grown using 15-min deposition times (60 min for the 10/400 film), and growth rates on a per-second and per-cycle basis were calculated using film thicknesses determined via profilometry. These results are summarized in Table I.

The growth rate per cycle increases slightly as off-time increases up to 100 ms. This is consistent with a significant proportion of deposition occurring during the off-time. As the off-time is increased beyond 100 ms, the growth rate per cycle decreases until it is almost negligible at 10/400 conditions. Similar trends are observed for film growth using other hydrofluorocompound (HFC) precursors. Figure 1 shows the growth rate per cycle as a function of off-time for three different HFC precursors—trifluoromethane (CHF$_3$), 1,1,2,2-tetrafluoroethane (C$_2$H$_2$F$_4$), and difluoromethane (CH$_2$F$_2$). The trend in growth rates for CHF$_3$ is very similar to that for CH$_2$F$_2$, which is not surprising given their chemical similarity. Similar mechanisms, such as HF elimination and carbene production, are likely to occur for all three precursors. However, CH$_2$F$_2$ does not show the same precipitous drop to near-zero film growth displayed by CHF$_3$ at 10/400 conditions; the reason for the observed difficulty in producing a stable 10/400 CHF$_3$ plasma is not known.

Although C$_2$H$_2$F$_4$ follows the same general trend as that of the other two precursors, growth rates are much higher for all off-times. The higher growth rates for C$_2$H$_2$F$_4$ can be explained, in part, by the fact that this precursor contains two carbons per molecule, allowing longer fragments to deposit compared to the other precursors, each containing only one carbon.[20] Additionally, the pulsed plasma process most likely dissociates the precursor molecules into reactive species with dif-

ferent efficiencies, and this is expected to have an effect on deposition rates.

Compared to the growth rate trends observed for films grown from these three HFCs, the trend in growth rate as a function of plasma off-time is qualitatively different for films grown from HFPO.[21] For HFPO, using a fixed on-period, the growth rate per cycle increases monotonically with off-time until approximately 200 ms and then plateaus at a constant value as off-time is increased further. This reflects the different processes which are likely to occur. In HFPO, HF elimination is not possible. In addition, the oxygen in this feed gas contributes substantially to the potential pathways available for reaction.

Film Composition

XPS

The relative proportions of different carbon-bonding environments were quantified by analysis of the C1s XPS peaks. The percentages of these different carbon-bonding environments are reported in Table II for the films grown at five different conditions. In general, the 10/20, 10/50, and 10/100 films display very similar chemical makeup, with about 37% of the carbon contained in CF$_2$ moieties. The 10/200 film, in contrast, shows a higher percentage of CF$_2$. This follows a trend observed with pulsed-plasma films grown from HFPO, where higher percentages of CF$_2$ are incorporated with a decreasing duty cycle.[12] In the limit of no plasma excitation, pyrolytic films grown from HFPO show very high percentages of CF$_2$, about 90%.[12]
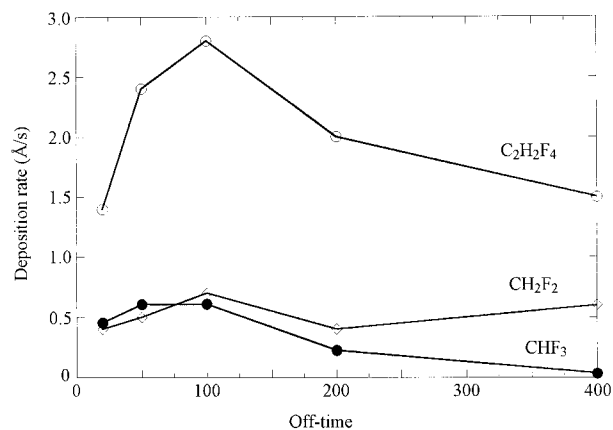

Figure 1   Growth rate per cycle as a function of plasma off-time for three different fluorocarbon precursors. Plasma on-time for all depositions was fixed at 10 ms. Data for CH$_2$F$_2$ and C$_2$H$_2$F$_4$ taken from ref. 20.

Table II   CHF$_3$ Film Composition

Plasma Conditions	% CF$_3$	% CF$_2$	% CF	% C—CF	F : C	Connectivity No.
10/20	14.4	37.3	23.2	25.0	1.41	2.41
10/50	15.6	37.3	20.8	26.3	1.42	2.48
10/100	15.8	36.5	21.8	25.9	1.42	2.46
10/200	11.6	47.7	17.6	23.1	1.48	2.40
10/400	14.7	32.2	21.7	31.3	1.30	2.55

Summary of $C1s$ XPS analysis of films grown from CHF$_3$ at five different sets of conditions. Percentages of the four different carbon bonding environments are listed. The F : C ratio and average connectivity number are calculated from the percentages, using the weighting methods of eqs. (1) and (2), respectively.

In addition, the F : C ratio and the connectivity number are reported in Table II. The F : C ratio is calculated from the percentages of different carbon environments as determined from the $C1s$ XPS by weighting each percentage by the number of F atoms bonded to that carbon. This is expressed in eq. (1):

$$F\text{:}C = \frac{(3 \times \% \ CF_3) + (2 \times \% \ CF_2) + (\% \ CF)}{100}$$

(1)

Bulk PTFE, having a molecular weight above 10^6,[22] is essentially composed of CF$_2$ units and thus has an F : C ratio of 2. In comparing pulsed-plasma fluorocarbon films, films with higher F : C ratios (approaching 2) are considered more "PTFE-like." The reproducible films grown from CHF$_3$ show F : C ratios of around 1.4–1.5, with the 10/200 film being the richest in fluorine at F : C = 1.48. The poorly-reproducible 10/400 film displayed a lower F : C ratio of 1.30.

The F : C ratio was also calculated from the atomic concentrations determined during the XPS survey scans of the five films. The F : C ratios calculated in this fashion evidenced the same trend as those calculated from the $C1s$ peaks, but were slightly higher in value—F : C values ranged from 1.60 for the 10/400 film to 1.82 for the 10/200 film. This disparity between F : C ratios calculated by the two different methods was observed by other workers.[23,24] In some of these cases, the F : C values calculated for fluorocarbon films or bulk PTFE from atomic concentrations sometimes substantially exceeded 2; this is impossible for PTFE (since high molecular weight PTFE has an F : C ratio of very nearly 2.0) and suggests using atomic concentrations to calculate F : C ratios is inaccurate. This inaccuracy was tenta-tively ascribed to errors in the instrument sensitivity factors.

The average connectivity number is a useful measure for estimating the rigidity of amorphous materials.[25,26] The connectivity number is the average number of network-forming bonds per atom. For our fluorocarbon films, it is calculated in a similar fashion to the F : C ratio, but the different carbon-bonding environments are weighted by their ability to bond to other carbons; bonds to F and H are ignored since these are terminal and will therefore not increase the network connectivity. If we also operate under the assumption that the percentage of carbon–carbon double bonds (i.e., sp^2 C) is minimal, the connectivity number, m, can be taken to be

$$m = \frac{\begin{array}{c}(\% \ CF_3) + (2 \times \% \ CF_2) + (3 \times \% \ CF) \\ + (4 \times \% \ C - CF)\end{array}}{100}$$

(2)

This assumption is most likely not strictly valid, since FTIR results (discussed below) suggest there is some double-bonded carbon in these films; however, this parameter is still useful for comparing pulsed-PECVD fluorocarbon films as they often display some sp^2 C character.

The percolation of rigidity for a system should occur at a connectivity value of 2.4; films with $m > 2.4$ are expected to be rigid (overconstrained), while films with $m < 2.4$ are expected to be flexible (underconstrained).[25,26] The films studied in this work all show values of m quite close to 2.4.

However, other evidence indicates that these films are brittle. Films of several micrometer thickness were deposited onto lengths of 75-μm diameter copper wire using the four stable sets of deposition conditions. Short lengths of these

Table III   Comparison of Film Compositions

Precursor	% CF_2	F : C	Connectivity No.
CF_3H	36	1.42	2.46
CH_2F_2	12	0.60	3.40
$C_2H_2F_4$	21	0.91	3.09
HFPO	55	1.78	2.22

% CF_2, F : C ratio, and connectivity number for 10/100 films grown from CHF_3 and three other precursors.[20,21] CHF_3 produces films that are richer in CF_2 than are the other fluorocarbon precursors, but not as CF_2-rich as are HFPO films.

coated wires were gently tied into loops of about 800 μm in diameter and inspected at various magnifications using an optical microscope. All four coatings exhibited delamination from the wire, indicating a brittle film.

Comparing 10/100 films grown from CHF_3 to 10/100 films grown from other precursor gases reveals a number of interesting facts (Table III). Trifluoromethane-derived films are more fluorine-rich than are films grown from the other two HFC precursors, CH_2F_2 and $C_2H_2F_4$, as evidenced by a substantially higher percentage of CF_2 and a higher calculated F : C ratio. In addition, the connectivity number is substantially lower for CHF_3 films. All three fluorocarbon precursors are inferior at producing fluorine-rich films when compared to HFPO, which has been shown to produce flexible wire coatings with high % CF_2 and corresponding lower connectivity number of $m = 2.1$.[4] Additionally, films grown from the HFC precursors all display higher proportions of quaternary carbon moieties (C—CF) compared to CF_3 and CF moieties, while films grown from HFPO show roughly equal distributions of CF, CF_3, and C—CF.[12,20]

FTIR

The FTIR spectra of the CHF_3 films provide a complementary means to probe film composition. The spectra of the different CHF_3 films display very similar features, and peak identities were assigned using IR peak information compiled by d'Agostino et al.[27a] The spectrum for the 10/20 film is shown in Figure 2. The prominent peak centered around 1230 cm^{-1} contains the very strong symmetric and asymmetric CF_2 stretches. The smaller peaks around this region are associated with CF_x moieties. The peak centered at about 1720 cm^{-1} generally indicates C=C and/or
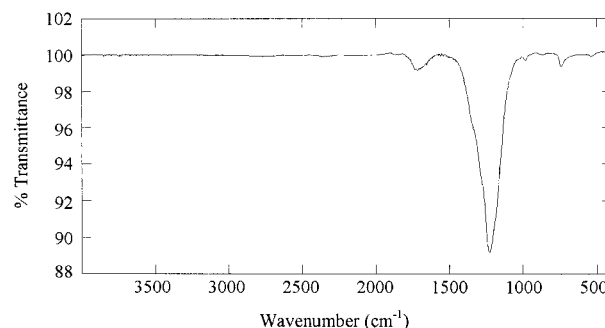

Figure 2   FTIR spectrum of 10/20 CHF_3 film. Main features are CF, CF_2, and CF_3 peaks. OH stretching around 3550 cm^{-1} is most likely due to adsorbed water. Spectra for CHF_3 films at lower duty cycles are similar but noisier due to lower film thickness.

C=O functionalities and is very often observed in pulsed-PECVD fluorocarbon films. The peak around 3500 cm^{-1} represents OH stretching and is most likely due to a small amount of adsorbed water. The lack of peaks around 2900 cm^{-1} indicates there is little, if any, hydrogen incorporated as C—H in these films. This spectral region is expanded in Figure 3, again for the 10/20 film.

In contrast, films grown from CH_2F_2 and $C_2H_2F_4$ both show C—H stretching peaks, indicating H incorporation into those films. This can be explained by considering the different breakdown mechanisms of these three HFC precursors. CHF_3 is known to break down predominantly into difluorocarbene (CF_2) and hydrofluoric acid (HF).[17,18] Thus, although CHF_3 is a fluorine-rich precursor (F : C = 3) that might be expected to have significant etching capability,[27b] the presence of hydrogen allows F atoms to be scavenged from the plasma via HF elimination.
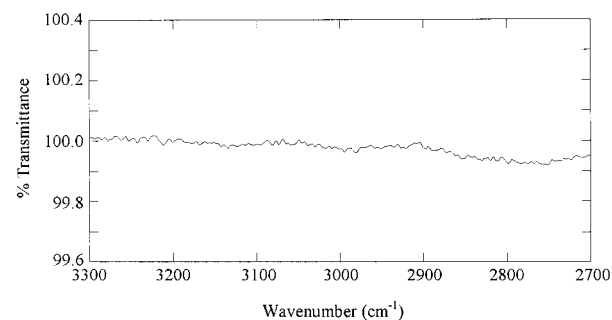

Figure 3   Expansion of FTIR spectrum of Figure 2 detailing CH_x stretching region of 10/20 CHF_3 film. No significant C—H incorporation into the film is observed. Spectra of other CHF_3 films are similar.
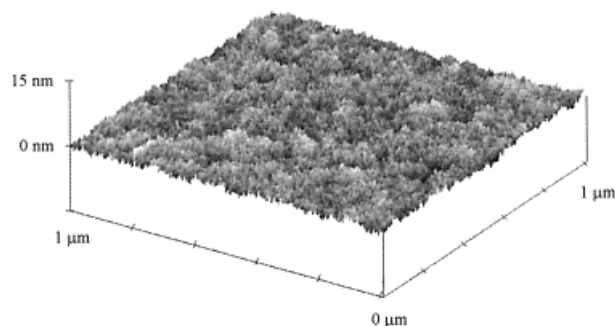
Figure 4 AFM image of 10/100 film grown from CHF$_3$. Film is about 5000 Å thick; area shown is 1×1 μm. Images of the other CHF$_3$ films are similar in appearance.

Figure 5 Surface roughness as a function of power factor, Q, for 10/100 films grown using three different fluorocarbon precursors. Data for CH$_2$F$_2$ and C$_2$H$_2$F$_4$ are taken from ref. 28.

CH$_2$F$_2$, on the other hand, breaks down to principally produce CHF and HF; although F can still be scavenged by HF elimination, CHF incorporation into the film provides a very substantial source of C—H. This helps account for the very low % CF$_2$ and F : C values observed for these films (see Table III). The breakdown of C$_2$H$_2$F$_4$ is somewhat more complicated; for a plasma on-time of 10 ms, it appears that this compound breaks down roughly equally via two pathways, one producing C$_2$HF$_3$ and HF and the other producing C$_2$F$_4$ (which can break down to two CF$_2$ units) and H$_2$.[28] The first route leads to substantial H incorporation, while the second produces CF$_2$-rich films. This explains why the C$_2$H$_2$F$_4$ film is intermediate in % CF$_2$ and F : C ratio compared to the CH$_2$F$_2$ and CHF$_3$ films (Table III).

AFM

The films grown from CHF$_3$ are intriguing in that they exhibit extremely low surface roughness as measured by AFM. Scans performed at three different resolutions for each film consistently yielded root-mean-square (rms) roughnesses of less than a nanometer, approaching the rms roughness value for the Si substrate, which was measured to be 0.53 nm.[29] The 1×1-μm AFM image of the 10/100 CHF$_3$ film is shown in Figure 4 and is typical of the AFM images of all the CHF$_3$ films; no large nodular structures are observed.

The subnanometer rms roughness observed for these films is substantially less than has been observed for comparable films grown from CH$_2$F$_2$ and C$_2$H$_2$F$_4$.[29] We believe an important contributing factor to the film roughness is the amount of plasma energy to which the growing film is subjected. This is quantified through the power fac-
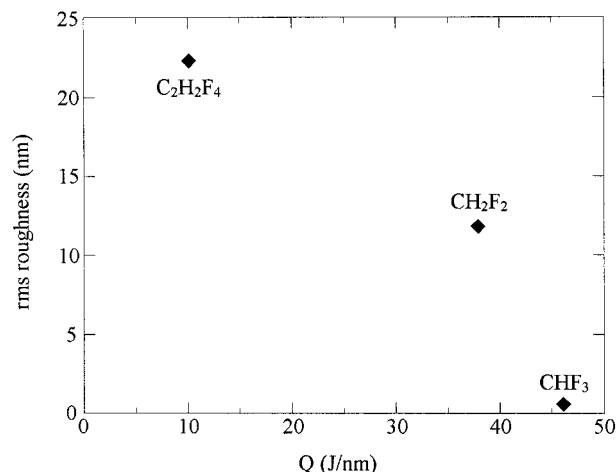
tor, Q, which is simply the plasma power input per cycle divided by the growth rate per cycle. Figure 5 plots the rms roughness of 10/100 films grown from the three HFC precursors as a function of Q. The slowest-growing film (from CHF$_3$) is subjected to the highest-power input and has the smoothest surface; the fastest growing film (from C$_2$H$_2$F$_4$) experiences the lowest-power input and has the roughest surface.

Table IV shows the rms roughness and power factor values for the five CHF$_3$ films, along with the film thickness. No clear trend in roughness with the power factor is observed for the CHF$_3$ films. This may be because the power factor Q may already be above a threshold value or that differences in surface roughness are hard to quantify so close to the roughness value for the Si substrate material.

Table IV   CHF$_3$ Film Roughness

Conditions	R_{rms} (nm)	Q (J/nm)	Film Thickness (nm)
10/20	0.786	61.7	1365
10/50	0.685	46.2	911
10/100	0.632	46.1	498
10/200	0.593	123	98
10/400	0.756	814	30

Roughness, power factor, and thickness of CHF$_3$ films grown at different plasma conditions. Values reported are for 1×1-μm scans; values obtained from 2×2-μm and 200 $\times$ 200-nm scans are very similar.

Wang and coworkers,[23] using a mixture of three C_9F_{18} olefins, deposited pulsed-PECVD fluorocarbon films on Si employing average powers similar to those used in this work. These films also displayed low surface roughness, ranging from 0.38 to 1.71 nm and F : C ratios ranging from 1.18 to 1.72.

Contact Angles

All the films were nonwetting, with advancing contact angles greater than 90°. The 10/20, 10/50, and 10/100 films gave contact angles of 109°; the 10/200 film an angle of 111°; and the 10/400 film an angle of 103°. Bulk PTFE displays a value of 108°.[30]

The contact angle is, in general, a function of both a surface's composition and roughness.[31] Since the surface roughness for these films is low and nearly constant, we believe that composition is the more important factor contributing to the small observed differences in contact angles. Increasing the number of fluorine atoms attached to a carbon center increases the group's hydrophobic nature. Increasing the hydrophobicity of the groups making up the surface will increase the contact angle; therefore, a film richer in CF_2 and CF_3 groups should evidence a higher contact angle than one richer in CF and quaternary carbon groups. The 10/20, 10/50, and 10/100 films have very similar proportions of CF_x groups and so, not surprisingly, yield the same contact angle value. The 10/200 film in comparison has a greater CF_2 fraction but lower CF_3, CF, and C—CF fractions. The net effect is a slightly more fluorinated film, reflected in the slightly higher F : C ratio. This is consistent with the slightly higher contact angle observed for the 10/200 film. Conversely, the 10/400 film is less fluorinated, with a lower F : C ratio, and the contact angle is lower. Figure 6 displays the advancing contact angles for the CHF_3 films as a function of the F : C ratio. These trends are consistent with work on pulsed-PECVD fluorocarbon films done by Wang et al.[23] who observed advancing contact angles with water to substantially increase as the F : C ratio increased, even while surface roughness slightly decreased.

Slightly smaller contact angles of 101° and 107° were observed for 10/100 films grown from CH_2F_2 and $C_2H_2F_4$, respectively. These films are substantially less fluorinated than were the CHF_3 films, but they are rougher (R_{rms} = 12 and 22 nm, respectively). Films grown from HFPO, in con-
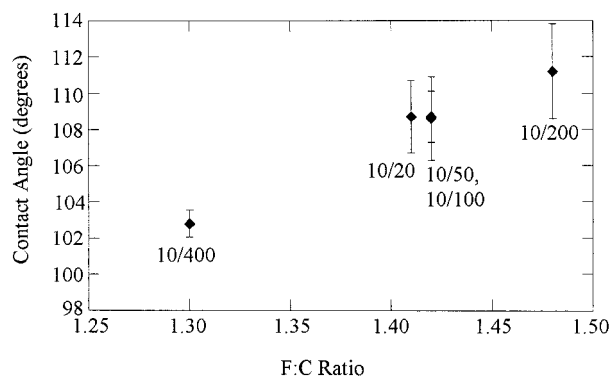

Figure 6 Advancing contact angle as a function of F : C ratio for films grown from CHF_3 (see also Table II).

trast, are more fluorinated and display a slightly higher contact angle, 113°, than that of the CHF_3 films.[29]

CONCLUSIONS

A series of fluorocarbon films was deposited onto Si substrates via pulsed-plasma enhanced CVD using trifluoromethane (CHF_3) as the source gas. Film compositions (as measured by changes in CF_x proportions) varied as the plasma duty cycle was changed (by varying the plasma off-time at a fixed on-time of 10 ms). The variation in CF_2 percentage was less pronounced for this precursor than has been observed for films grown from HFPO under similar conditions. We believe this is due to CHF_3 decomposition being dominated by one pathway, breaking down predominantly to produce CF_2 and HF, therefore making it difficult to alter ratios of these two gas-phase species via plasma conditions.

The films display an F : C ratio of 1.4–1.5, substantially higher than observed for films grown from two other HFC precursors, CH_2F_2 (film F : C = 0.60) and $C_2H_2F_4$ (film F : C = 0.91); films from HFPO show a higher ratio (film F : C = 1.78). In addition, the average connectivity number for CHF_3 films is about 2.4, considered the value where percolation of rigidity can occur and films can become flexible; this is significantly lower than the average connectivity value observed for the other HFC precursors. However, optical microscopy of loops of coated wires reveals delamination of the films, indicating that the deposited films are rigid. Films grown from HFPO have displayed lower average connectivity num-

bers ($m = 2.2$) and flexible characteristics when coated onto wires and tied into loops.

FTIR spectra indicate that the films are essentially composed of CF_x species and that there is very little C—H incorporation into films grown using CHF_3 at any of the plasma conditions. Films grown from CHF_3 are extremely smooth, with rms roughnesses (determined by AFM) on the order of the roughness of the Si wafer substrate, about 0.5 nm. We believe this is due in large part to the relatively low film growth rates, which result in a large amount of plasma power being applied to the growing film.

Advancing contact angles with water are close to 108°, the value for bulk PTFE. A very small trend in the contact angle with a varying duty cycle is observed, with more fluorinated (higher F : C ratio) films displaying higher contact angles, that is, exhibiting a more nonwetting, hydrophobic character.

REFERENCES

1. Endo, K.; Tatsumi, T. J Appl Phys 1995, 78, 1370–1372.
2. Endo, K. MRS Bulletin 1997, 22(10), 55–69.
3. Labelle, C. B.; Limb, S. J.; Gleason, K. K.; Burns, J. A. In Proceedings of Third International Dielectrics for ULSI Multilevel Interconnection Conference (DUMIC), 1997; pp 98–105.
4. Limb, S. J.; Gleason, K. K.; Edell, D. J.; Gleason, E. F. J Vac Sci Technol A 1997, 15, 1814–1818.
5. Yasuda, H.; Gasicki, M. Biomaterials 1982, 3, 68–77.
6. Gumbotz, W. B.; Hoffman, A. S. CRC Crit Rev Biocompat 1987, 4, 1–42.
7. Grischke, M.; Bewilogua, K.; Trojan, K.; Dimigen, H. Surf Coat Technol 1995, 74–75, 739–745.
8. Pittman, A. G. In Fluoropolymers; Wall, L. A., Ed.; Wiley: New York, 1972; Vol. 25, p 419.
9. Momose, Y.; Takada, T.; Okazaki, S. In Proceedings of the ACS Division of Polymeric Materials, Polymeric Materials Science and Engineering. CF4 and C2F6 Plasma Fluorination of Hydrocarbon and Fluorocarbon Polymers, Denver, CO, 1987; p 236.
10. Labelle, C. B.; Gleason, K. K. In ECS Symposium Proceedings, First International Symposium on Environmental Issues with Materials and Processes for the Electronic and Semiconductor Industries. Environmental, Safety, and Health Issues Associated with Low Dielectric Constant Films Grown by Chemical Vapor Deposition, San Diego, 1998; pp 27–34.
11. Savage, C. R.; Timmons, R. B.; Lin, J. W. Chem Mater 1991, 3, 575–577.
12. Limb, S. J.; Lau, K. K. S.; Edell, D. J.; Gleason, E. F.; Gleason, K. K. Plasmas Polym, in press.
13. Labelle, C. B.; Lau, K. K. S.; Gleason, K. K. Mater Res Soc Symp 1998, 511, 75–86.
14. Millward, G. E.; Hartig, R.; Tschuikow-Roux, E. J Phys Chem 1971, 75, 3195–3201.
15. Burgess, D. R., Jr.; Zachariah, M. R.; Tsang, W.; Westmoreland, P. R. Prog Ener Combust Sci 1996, 21, 453–529.
16. Limb, S. J.; Labelle, C. B.; Gleason, K. K.; Edell, D. J.; Gleason, E. F. Appl Phys Lett 1996, 68, 2810–2812.
17. Schug, K. P.; Wagner, H. G.; Zabel, F. Ber Bunsenges Phys Chem 1979, 83, 167–175.
18. Hidaka, Y.; Nakamura, T.; Kawano, H. Chem Phys Lett 1991, 187(1,2), 40–44.
19. Limb, S. J.; Edell, D. J.; Gleason, E. F.; Gleason, K. K. J Appl Polym Sci 1998, 67, 1489.
20. Labelle, C. B.; Gleason, K. K. J Vac Sci Technol A 1999, 17, 445–452.
21. Limb, S. J. PhD Thesis, Massachusetts Institute of Technology, 1997.
22. Organofluorine Chemicals and Their Industrial Applications, Banks, R. E., Ed.; Wiley: New York, 1979; p 238.
23. Wang, J.-H.; Chen, J.-J.; Timmons, R. B. Chem Mater 1996, 8, 2212–2214.
24. Clark, D. T.; Shuttleworth, D. J. J Polym Sci Polym Chem Ed 1980, 18, 27.
25. He, H.; Thorpe, M. F. Phys Rev Lett 1985, 54, 2107.
26. Dohler, G. H.; Dandoloff, R.; Bilz, H. J Non-Cryst Solids 1980, 42, 87.
27. (a) d'Agostino, R.; Cramarossa, F.; Fracassi, F. In Plasma Deposition, Treatment, and Etching of Polymers, d'Agostino, R., Ed.; Academic: San Diego, 1990; pp 95–162; (b) p 98.
28. Labelle, C. B.; Karecki, S. M.; Reif, L. R.; Gleason, K. K. submitted for publication in J Vac Sci Technol A.
29. Labelle, C. B.; Gleason, K. K. J Appl Polym Sci, in press.
30. Zisman, W. A. Adv Chem Ser 1964, 43, 1.
31. Adamson, A. W.; Gast, A. P. Physical Chemistry of Surfaces, 6th ed.; Wiley: New York, 1997; Chapter 10.